Nuclear-quadrupole-resonance study of the 145-K charge-density-wave transition in $NbSe_3$

B. H. Suits* and C. P. Slichter
Physics Department and Materials Research Laboratory, University of Illinois at Urbana—Champaign, Urbana, Illinois 61801
(Received 13 June 1983)

The authors have used spin echoes to study the ^{93}Nb nuclear-quadrupole-resonance (NQR) line shapes and relaxation times in $NbSe_3$ through the charge-density-wave transition at 145 K. Of the 12 NQR lines present above 145 K, arising from the three different Nb sites each of which contributes four NQR lines, only six were observed in the frequency range studied. The authors have determined that these six lines arise from two distinct quadrupole fields with one axial or nearly axial ($\eta \simeq 0$) and the other nearly "antiaxial" ($\eta \simeq 1$). A simple argument suggests that these two sites are the ones which appear most similar in the crystal structure. Below 145 K the nearly axial line becomes nonaxial ($\eta = 0.55$) while the nearly antiaxial line smears slightly. Relaxation data combined with the line-shape data show that dynamical effects are present at the nearly axial site and the changes in the spectra may be due principally to a change in the dynamics of the quadrupole field at that site. Dynamics are relatively unimportant at the antiaxial site. The third site has yet to be observed.

I. INTRODUCTION

The metallic linear-chain compound niobium triselenide, $NbSe_3$, has been found to exhibit unusual properties which have been associated with the formation of charge-density waves (CDW's). Reported here are the results of a nuclear-quadrupole-resonance (NQR) study of this compound undertaken in an effort to understand more fully the origin of these unusual properties and their relationship to the CDW's.

$NbSe_3$ exhibits a large increase in the electrical resistivity below each of two transition temperatures, 145 and 59 K.[1,2] Diffraction results show that below each of these temperatures a periodic lattice distortion (PLD) develops, in addition to a CDW, in a continuous way, each with a wavelength which is incommensurate with the lattice periodicity.[3–5] It is also found that when the CDW's are present the conductivity becomes non-Ohmic[6] for electric fields above a threshold field E_T.[7–9] The frequency dependence of the conductivity shows a strikingly similar behavior above a threshold frequency ω_T.[10] In the limit of high electric fields or high frequencies the resistivity appears to have the temperature dependence that one would expect if the CDW's were not present.[6–10] However, x-ray-diffraction results both with and without an applied electric field[5] reveal no change in the CDW amplitude or wavelength. These results have lead to the hypothesis that the CDW can move or "slide" under an applied electric field as discussed some time ago by Frohlich.[11] The only direct evidence thus far for CDW motion of any kind appears in the results of Fung and Steeds[12] where dynamics were observed in images obtained using an electron microscope (without an intentionally applied field).

The structure of $NbSe_3$ is monoclinic and consists of three chains or columns each of which is represented twice in a unit cell.[13] Following Wilson[14] we will label them as red, yellow, and orange. The yellow and orange chains, though distinct, are relatively similar and appear to exhibit strong Se-Se pairing while the red chains do not. Wilson presents a simple picture of how the incommensurate CDW may manifest itself in a quasicommensurate way and postulates that the transitions at 145 and 59 K are predominantly due to the yellow and orange chains, respectively. Bullett[15] has calculated a band structure for $NbSe_3$ which supports Wilson's hypothesis on the basis of the favorability of Fermi-surface nesting and the observed CDW wavelengths. We will show that the CDW transition is somewhat more complicated than this simple picture would predict. Both of the sites we observe show changes at the transition and the changes for the two sites are very different in nature.

In this paper are reported the results of an NQR study, utilizing the ^{93}Nb nucleus ($I = \frac{9}{2}$), of the formation of the CDW below the upper transition. This work was undertaken in an effort to obtain a detailed microscopic look at the formation and dynamics of the CDW which appears below 145 K. While much of the published work on this compound has been done below the 59-K transition due to the smaller thresholds for non-Ohmic conduction, the interpretation of NQR spectra is greatly facilitated by remaining above 59 K where only one CDW is observed. In all the measurements reported here no electric field was applied and the frequency of operation was below the threshold frequency ω_T.

In Sec. II the theory of the electric quadrupole coupling is reviewed briefly to set the stage for what follows. Section III discusses the experimental aspects of this work with the results presented and discussed in Sec. IV. Section V serves as a summary.

 ©1984 The American Physical Society

II. ELECTRIC QUADRUPOLE INTERACTIONS: ELECTRIC QUADRUPOLE FIELD

The electric quadrupole field has been discussed by many authors[16–19] and will only be reviewed here briefly for the sake of clarity. The quadrupole Hamiltonian can be written[19]

$$H_Q=\frac{eQ}{6I(2I-1)}\sum_{i,j}V_{ij}[\tfrac{3}{2}(I_iI_j+I_jI_i)-\delta_{ij}I^2]\,, \quad (1)$$

where Q is the quadrupole moment of the nucleus with spin I, V_{ij} is an element of a traceless second-rank tensor describing the quadrupole field at the nucleus, and I_i and I_j $(i,j=x,y,z)$ are the usual angular-momentum operators. If the axes used yield $V_{ij}=0$ for all $i\neq j$, a particularly convenient choice, they are referred to as principal axes. In that case the Hamiltonian takes the form

$$H_Q=\frac{e^2Qq}{4I(2I-1)}[(3I_z^2-I^2)+\eta(I_x^2-I_y^2)]\,, \quad (2)$$

where $eq=V_{zz}$ and $\eta=(V_{xx}-V_{yy})/V_{zz}$. The parameter η is referred to as the asymmetry parameter. There are two highly symmetric types of quadrupole fields, the axial case $(\eta=0,\pm3)$ which has the rotational symmetry of $3z^2-r^2$ and the antiaxial case $(\eta=\pm1,\infty)$ which has the rotational symmetry of x^2-y^2. It is usual to choose the coordinate axes which give $0\leq\eta\leq1$ which is equivalent to saying $|V_{xx}|\leq|V_{yy}|\leq|V_{zz}|$. This provides a unique choice of coordinates for any static quadrupole field.

With a powder sample only e^2qQ and η can be measured directly. The direction(s) of the principal axes are unknown. For the case of $NbSe_3$ the room-temperature structure data indicate a mirror plane through each Nb site and perpendicular to the b axis.[4] This would imply that at room temperature one of the principal axes for each site lies along the b axis.

In what follows it will be convenient to express the quadrupole coupling in units of

$$\nu_Q=3e^2qQ/[2I(2I-1)h]\,,$$

where h is Planck's constant. The quadrupole-split nuclear energy levels can be readily calculated numerically using Eq. (2) or one can use the tabulated results of Cohen.[18] The energy levels and the resultant transition frequencies for $I=\frac{9}{2}$ are shown in Fig. 1 for different values of η. The *labels* for the energy levels are those of Cohen. For nonzero values of η virtually all magnetic dipole transitions, which are what we observe with an NQR measurement, become allowed. However, in most cases where the label m changes by more than 1 ("forbidden transitions") the signal is too weak to observe. The dashed lines in Fig. 1 indicate the most observable of the forbidden transitions.

The origin of the quadrupole field seen by a nucleus is typically divided into two parts: the contribution from the valence electrons immediately surrounding the nucleus, V_{local}, and the contribution of the surrounding lattice (e.g., the other nuclei plus electrons not at the site in question), V_{lattice}.[17,20] Associated with each is a shielding (or antishielding) factor which reflects the degree to which the electrons, as a whole, distort in the presence of the electrostatic field and provide a proportionate field of their own. The total quadrupole field is typically written as

$$V=(1-\gamma_\infty)V_{\text{lattice}}+(1-R)V_{\text{local}}\,, \quad (3)$$

where γ_∞ for Nb has been calculated[21] to be -15 and R is typically 0.1. In a metal an additional complication may arise since the conduction electrons may contribute to both the local and lattice terms.[17] In what follows no attempt will be made to separate the two types of contributions as such an attempt would be futile at this time without more detailed knowledge of the electronic wave functions, in particular, how the charges are distributed among the selenium sites. However, in niobium *di*selenide, $NbSe_2$, calculations show that the lattice contribution is negligible[20,21] and it thus seems reasonable that this might also be so in $NbSe_3$.[22] This assumption is implicit in some of the discussion which follows with the realization that what seems reasonable need not be true.

In the Appendix the results of a calculation of the local contribution to the quadrupole field is presented in some detail. It is important to note that the symmetry of the quadrupole field does not necessarily reflect the full symmetry of the total electronic charge but only those parts which transform under rotations as the spherical harmonics, Y_2^m. Thus, even though the niobium sites in $NbSe_3$ have very little symmetry associated with them, the quadrupole field may have, or, in some sense, be close to having, a high degree of symmetry.

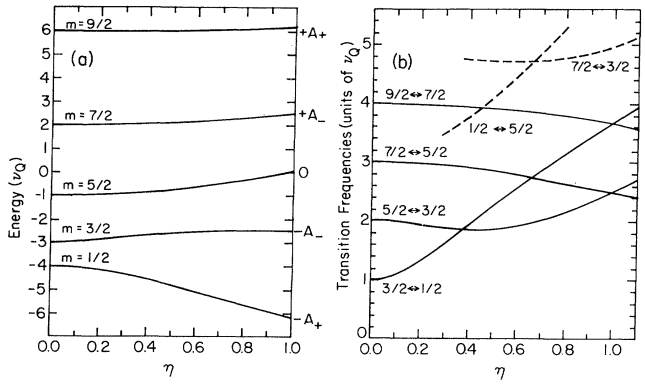

FIG. 1. (a) Nuclear energy levels and (b) transition frequencies for a nucleus with spin $I=\frac{9}{2}$ in the presence of a quadrupole field characterized by ν_Q and η. Here $A_\pm=(22\pm\sqrt{748/3})^{1/2}$.

III. EXPERIMENTAL

A. Samples

The $NbSe_3$ samples used in this study were grown from a stoichiometric mixture of niobium and selenium in an

evacuated, sealed quartz tube. The tube was placed in a temperature gradient of about 40 °C with the hot end just below 700 °C. The reactants were placed at the hot end of the tube and the crystals grew at the colder end. This process yields a large number of relatively thin (typically 0.1×0.01 mm^2) crystals which varied in length from about 1 to over 5 cm. The electrical resistance of a large number of crystals from several batches arranged in parallel was measured. These data are shown in Fig. 2 and agree very well with previously published data.[1,2]

The NMR sample was prepared using crystals from several growth batches mixed with alumina powder. The alumina acts as an electrical insulator between the crystals and greatly reduces losses due to eddy currents induced in the sample by the applied rf field used in NQR experiments. This method greatly increases the NQR sensitivity relative to using the same sample without the alumina. The sample then consists of many small single crystals with random orientations. Interference from the NQR signal of the ^{27}Al in the alumina is not present in the frequency range we have studied.[23]

B. NQR experiments

Most of the results we present were obtained using a two-pulse NQR sequence resulting in a signal known as a spin echo. Since the signals are quite weak extensive signal averaging of typically 50 000 echoes was necessary. With this much averaging any extraneous coherent signals, such as signals from the recovery of the probe after the relatively large rf pulse, can completely mask the signal. To eliminate these problems the pulse sequence actually used, illustrated in Fig. 3(a), alternately provides a positive and a negative incoming spin-echo signal.[24] After digitization the incoming signal is then alternately added to or subtracted from the accumulated sum. Since the extraneous signals due to the recovery of the probe are primarily due to the second pulse, which is the same in both cases, they will cancel while the NQR signals add.

There are three times present in this pulse sequence which can be varied independently. For a narrow, spin $I=\frac{1}{2}$ NMR resonance (in a magnetic field) the integrated spin-echo intensity obtained using this sequence, $S(\tau,t_d,t_{\rm rep},\omega)$, can be shown to vary approximately as

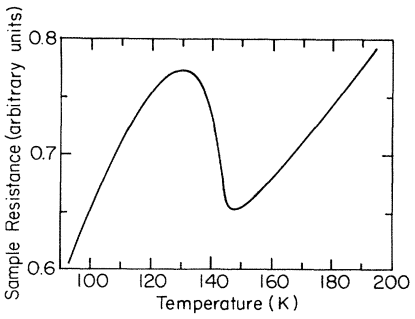

FIG. 2. Sample resistance for approximately 200 crystals arranged in parallel as a function of temperature.

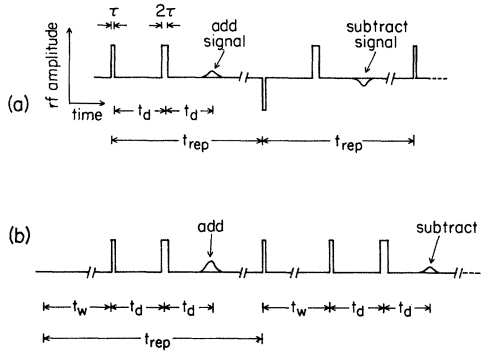

FIG. 3. NQR pulse sequences used (a) for line-shape and T_2 measurements and (b) for measurements of T_1. Spin-echo signal is roughly 9 orders of magnitude smaller than the pulse height.

$$S(\tau,t_d,t_{\rm rep},\omega)\propto\gamma\sin^3(\gamma H_1\tau)\exp(-2t_d/T_2)\times[1-\exp(-t_{\rm rep}/T_1)]f(\omega)\,, \tag{4}$$

where γ is the gyromagnetic ratio, H_1 is the amplitude of the applied rf field, T_2 is the "spin-spin" relaxation time, T_1 is the spin-lattice relaxation time, $f(\omega)$ is a line-shape function, and ω is the frequency of the rf field. The maximum signal is obtained when $\gamma H_1\tau=\pi/2$.

For the case studied here, principally NQR powder spectra, where we are observing only a single of the many possible transitions, the mathematics can be shown to be that of the spin-$\frac{1}{2}$ problem with only minor modifications.[25,26] Treating the problem as an ensemble of experiments with fixed quadrupole axes and a distribution of directions for the rf field, one has the approximate relation for the transition between states labeled m and m',

$$S(\omega)\propto\int_0^\infty d\omega_1 g(\omega_1)\omega_1\sin^3(\omega_1\tau)F(t_d/T_2)\times[1-G(t_{\rm rep}/T_1)]f(\omega)\,, \tag{5}$$

where $\omega_1=\gamma H_1\,|\,\langle m\,|\,\vec{\mathrm{I}}\,|\,m'\rangle\,|$, $g(\omega_1)$ is the distribution function for ω_1 due to the average over angles between the applied field and the quadrupole axes, and F and G are functions at least qualitatively similar to the corresponding exponentials in Eq. (4).

For an axial quadrupole field and a powder average, $g(\omega_1)$ is a constant up to a maximum value $\omega_{\rm max}$, then is zero for greater value. For nonaxial quadrupole fields one can calculate $g(\omega_1)$ for a powder quite readily starting from the results of Bloembergen and Rowland.[27,28] Empirically one has the result that the maximum signal corresponds to $\omega_{\rm max}\tau\approx2\pi/3$. Thus by varying the pulse length τ one can determine, in principle, to which states m and m' correspond.

By varying t_d and $t_{\rm rep}$ one can obtain a measure of T_2 and T_1, respectively. This works well for T_2 measurements; however, for short values of T_1 it becomes impractical to vary the repetition time $t_{\rm rep}$. For T_1 measurements we added a third pulse on every other cycle, as is shown in Fig. 3(b), a time t_w before the τ pulse. The resul-

tant signal is the difference between the signals with and without the new pulse. For long times, $t_w \gg T_1$, the nuclei have fully recovered from the new pulse and the resultant difference is zero. For shorter times the signal from the second set of pulses is smaller than that from the first so a net signal is obtained. The size of this signal as a function of t_w gives a measure of the spin-lattice relaxation time T_1.

NQR line shapes for $NbSe_3$ were generated point by point. Each point represents the area under the spin-echo signal measured at a given frequency. The only narrow-band components in the spectrometer were the probe ($Q \approx 50$) and several quarter-wavelength cables used in a passive transmit-or-receive switch. The probe was retuned each time the frequency was altered while the cables were changed only for large changes in frequency. Five sets of cables covered the range between 2.5 and 5.3 MHz quite satisfactorily.

The hydrogen NMR signal at room temperature from a sample containing a mixture of glycerin and doped water showed that the magnitude of the rf field (H_1) was roughly 25 G and varied little over the frequency ranges studied.

For the sake of consistency all measurements of the line shape were done with a pulse length τ of 2 μs. This pulse length does not optimize the intensity for all of the transitions observed. The delay time t_d was 150 μs throughout the line-shape study.

Because of the relatively large frequency and temperature range studied, each point of the line shape was multiplied by the temperature T and divided by the frequency $F = \omega/2\pi$ to correct for changes in intensity due to the changing Boltzman factor (in the high-temperature limit), which is not of interest here.

Temperatures were measured using a silicon diode and a constant-current source. The same diode was used for the resistance and the NQR measurements. The absolute calibration of the diode is no better than ± 1 K with a resolution of much better than 0.1 K. The temperature was stabilized to better than 1 K for all the data and to better than 0.1 K for the data between 130 and 146 K.

It is worthwhile to point out that while the frequency of the rf field used here is always below the threshold frequency for non-Ohmic conduction, one has electric fields induced in the samples by the oscillating magnetic field. With the use of relatively simple arguments[29] one can estimate the size of the induced field. For $NbSe_3$ crystals with crosswise dimensions larger than the skin depth (~ 0.5 mm) one obtains a maximum induced electric field of about 0.1—0.3 V/cm, or roughly the value for the threshold field seen by Gill.[10] However, all the crystals used in the NQR study are thinner than the skin depth and relatively few will have the orientation which gives rise to the maximum field. Thus this maximum field is not achieved and the data presented here represent the sample within its Ohmic region.

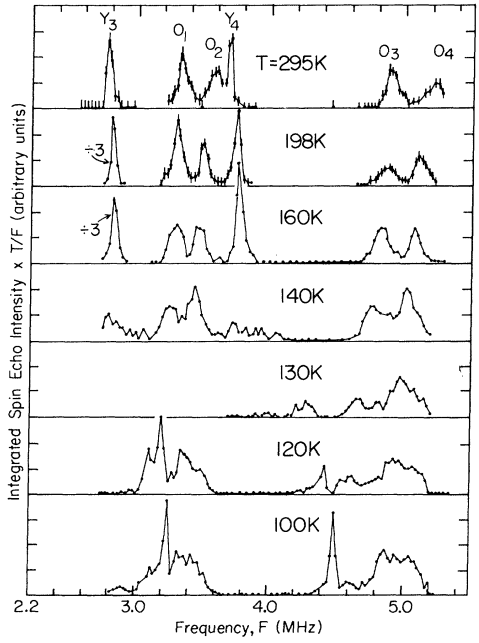

FIG. 4. NQR line shapes for $NbSe_3$ for various temperatures between 100 and 295 K.

IV. RESULTS AND DISCUSSION

A. Line shapes

NQR line shapes of $NbSe_3$ were measured between 2.6 and 5.3 MHz for several temperatures between 100 and 300 K. The results are summarized in Fig. 4. The labeling of the peaks will be discussed later. The line shapes from the higher temperatures (greater than 145 K) correspond to the normal state and will be discussed first followed by a discussion of the line shapes with CDW present.

B. Normal state

Above 145 K no PLD is observed in diffraction studies and no anomalies are observed in the conductivity. The line shape for temperatures above 145 K should then reflect this "normal" state. The line shapes above 145 K show six peaks. Since there are three different types of Nb sites in the unit cell and each contributes four NQR lines, there are six lines which are unaccounted for. These missing lines may be under another line, out of the frequency range measured, and/or they may have a very long spin-lattice relaxation time T_1 and are thus unobserved [see Eq. (4)]. With the use of the observed lines alone one cannot uniquely fit the data with a set of three quadrupole fields. Further considerations are thus necessary to understand the normal-state spectrum.

By considering the temperature dependence of the line positions we find a correlation between the first three lines from the left in Fig. 4 and the last three (in the same order). The first and fourth lines have frequencies in a ratio of 1.33 ± 0.01:1 for all temperatures studied above 145 K. There are many possible quadrupole fields which give this ratio, one of which corresponds to $\eta \simeq 0$. Fields other than

axial or nearly axial show a strong change in the ratio of the frequencies with only a slight change in η. Since with the exception of high-symmetry cases one expects η to change with temperature, it is concluded that these two lines correspond to the two highest-frequency lines of an axial or a nearly axial quadrupole field. While there is only 1% error in the frequency ratio the best we can claim for η is $0 \leq \eta \leq 0.25$. The value of η can be determined more precisely by observing the lower-frequency transitions. In the remainder of this paper the term "nearly axial" should be understood to include the exactly axial limit $\eta = 0$.

The remaining four lines occur as two closely spaced pairs. The ratios of the frequencies of the highest of each pair to that of the lowest of each pair are both 1.46 ± 0.02, again relatively independent of temperature. In this case the lack of temperature dependence points to the antiaxial case $\eta \simeq 1$. One cannot tell whether there are two sites present with $\eta = 1$ or one type of site with $\eta \approx 0.95$ (refer to Fig. 1).

Judging from the crystal structure[4] and the band structure[15] one expects the yellow and orange chains to be relatively similar while the red chains may be quite different from them. One might then conclude that there are two similar sites with $\eta = 1$ and the axial field corresponds to the red site. However, measurements of the matrix element ω_{max} (Ref. 26) and comparison of the intensity of these lines with the nearly axial lines already discussed suggests the four lines arise from one site with $\eta = 0.95$. Since these measurements may be unreliable for these spectra due to the size of the rf field compared to the linewidth and uncertainties in short-time relaxation phenomena, an unambiguous test of this assignment was pursued. Such a test is to observe the frequency of the forbidden transition(s) $m = \frac{7}{2} \leftrightarrow m = \frac{3}{2}$ (refer to Fig. 1). One will either see two lines each appearing at exactly twice the frequency of the corresponding line in the lower-frequency pair for the case of two sites, or only one line at a frequency equal to the sum of the frequencies of the two lines in the lowest pair for the case of one site with $\eta \approx 0.95$. [Of course, one could also have two sites with the same value of η_Q and η ($\eta \approx 0.95$). In light of the crystallographic and electronic differences between the three sites and again considering the relative intensities of the NQR lines this is considered unlikely.]

Measurements at 195 K, shown in Fig. 5, show a single forbidden transition at the sum frequency. Thus the two pairs of lines arise from a single quadrupole field.

The assignments of the quadrupole-field values were also checked by varying the pulse length as discussed in Sec. III. The uncertainty of these measurements of the maximum matrix element ω_{max} is about 20%, which is not good enough to label all of the lines; however, one can distinguish the highest-frequency (allowed) transitions—or highest two for $\eta \simeq 1$—from the others. The results further confirmed the above assignments.

We conclude that the six lines we observe arise from two quadrupole fields—one nearly axial and one nearly "antiaxial." The parameters ν_Q and η plotted as a function of temperature for these two quadrupole fields are shown in Fig. 6. The third site was not observed.

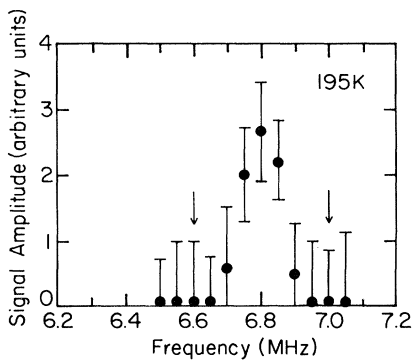

FIG. 5. $\frac{7}{2} \leftrightarrow \frac{3}{2}$ forbidden transition. Arrows indicate the frequencies where the lines would be observed if two sites with $\eta = 1$ are present.

An attempt was made to observe the third site through the use of a strong static magnetic field (e.g., an NMR experiment). In this case the frequency was held constant (72.859 MHz) while the field was changed. Spin echoes were recorded digitally as the magnetic field was linearly swept.[30] The repetition time t_{rep} used here was 10 ms. The spectra are experimentally broadened by about 30 G by the signal-averaging program. The line shape observed is shown in Fig. 7(a).

Aside from sharp edges the NMR spectrum is quite featureless. A theoretical powder pattern calculated using first-order perturbation theory[27,28] (second order for the central transition[31]) and the values for the two quadrupole fields observed with no magnetic field is shown in Fig. 7(b). The relatively close agreement between the theory and the experiment is surprising since the third-site and Knight-shift interactions, both of which should be present in the experimental results to some degree, are not included in the theory. More conclusive results should be obtainable through the use of a carefully aligned sample; we have, however, not pursued this approach.

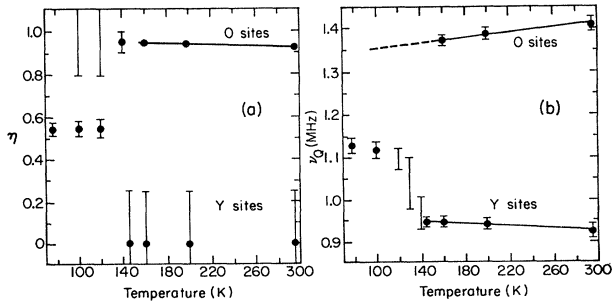

FIG. 6. Values for the (a) symmetry parameter η and (b) quadrupole coupling constant ν_Q for the two observed sites as a function of temperature.

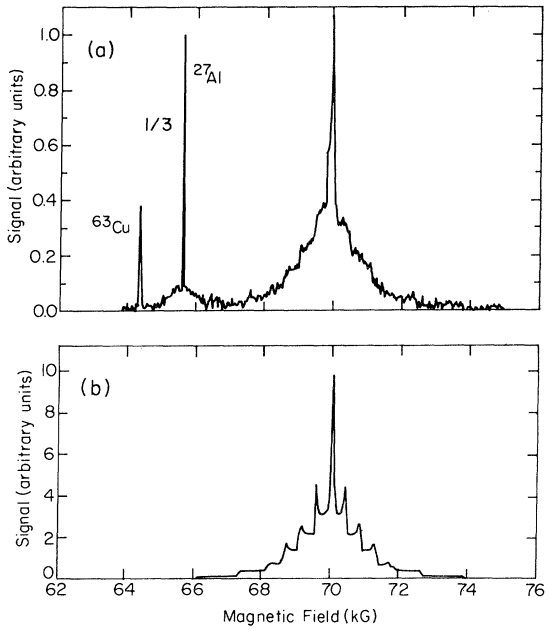

FIG. 7. (a) NMR line shape of $NbSe_3$ at room temperature at a frequency of 72.859 MHz as a function of the magnetic field. Aluminum signal arises from the alumina mixed with the sample and the copper signal is most likely from the brass coil used for these measurements. (b) Theoretical NMR line shape using parameters obtained from the NQR data.

We can conclude from the magnetic field study that on the whole the Knight shifts are relatively small (0.1—0.2 %) for all the sites observed, or roughly half the values observed in $NbSe_2$.[32,33] The slight asymmetry in the NMR spectrum is probably due to a nonisotropic Knight-shift interaction. A nonisotropic Knight shift will smear the peaks (singularities) in the theoretical line shape with the peaks near the center smeared more than the peaks farther out. The third site presumably has a spin-lattice relaxation time T_1, which is longer than 10 ms under the conditions of the measurement, making it difficult to observe.

Now, going back to the NQR data, we would like to attempt to label the quadrupole fields observed in terms of the sites in the crystal structure. That is, using Wilson's terminology,[14] label the fields red, orange, or yellow. With the use of the fact that the environments immediately surrounding the Nb atoms in $NbSe_2$ and $NbSe_3$ are somewhat similar and that the quadrupole field is proportional to the local density of conduction electrons, we can estimate the quadrupole field for each site. Bullett[15] has estimated that there are 0.1, 0.8, and 1.1 electrons per unit cell for the red, yellow, and orange chains, respectively. By scaling the quadrupole field observed by Chen[34] in $NbSe_2$ ($\nu_Q = 2.58$ MHz at 77 K), where there is one conduction electron per niobium, atom one obtains $\nu_Q = 0.13$, 1.03, and 1.42 MHz for the red, yellow, and orange chains, respectively. We will use the correlation of the calculated values with the measured values (Fig. 6) to obtain *tentative* identification for the lines in the NQR line shape. We label the observed NQR lines by the letters *O* and *Y*, assigning *O* and *Y* to what we believe tentatively are Wilson's orange and yellow sites, respectively. These calculated values suggest that the unobserved (red) site has a relatively small quadrupole field.

It is somewhat puzzling at this point as to why the quadrupole fields at the *Y* and *O* chains should have such different symmetries when the crystal structure indicates they should be similar. Possible resolutions of this question will be presented later in this paper.

C. CDW state

The changes in the spectra below 145 K reflect the influence of the CDW on the NQR spectrum. Both the orange and yellow chains appear to be affected though in different ways.

The lines we have associated with the orange chains (see Fig. 4) broaden a bit as the transition approaches, then below the transition a small portion of the line splits off in a continuous way to form a broad background which is easily saturated (T_1 long). The lines are too broad and lacking in structure to attempt to analyze them further. We make three qualitative observations. First, the change in the line shape is gradual and is not particularly large. Second, the temperature dependence of the center of gravity of the lines appears to be relatively unaffected by the transition. These first two observations are what one might expect to see in the presence of an incommensurate CDW. Third, the line shape at 100 K is not what one would expect for either a singly incommensurate plane-wave modulation[35] or the quasicommensurate model discussed by Wilson.[14] Each of these two models would give the appearance of splitting each line in the spectrum into two lines, though a detailed line-shape measurement should distinguish between them.

The change in the lines we have associated with the yellow chains is much more pronounced. The lines appear to sweep across in frequency to a new set of narrow lines with $\eta = 0.55$ and a new value of ν_Q, 1.12 MHz. Since the lines virtually disappear in the process one cannot tell if all of the yellow sites move to this new value. Based on intensity measurements it appears that at least a large fraction of the sites have moved to this new value.

That there appears to be only a single quadrupole field associated with these new lines suggests one or more of the following.

(i) There is no measurable periodic modulation associated with the *Y* sites.

(ii) There is a periodic modulation but it is a modulation in the crystallographic orientation of the quadrupole axes and not in ν_Q or η.

(iii) The periodic modulation is moving rapidly so that only an average quadrupole field, the same for all nuclei, is observed.

(iv) The effects of the modulation on the quadrupole field are such that some fraction of the nuclei become unobservable and thus it is a single narrow line only in appearance.

Bardeen has pointed out to us that thermal excitation could lead either to depinning of the CDW's if they are sufficiently weakly bound, or to large-scale oscillations (several lattice distances in amplitude) at somewhat lower temperatures or for more strongly bound CDW's. Either mechanism could explain case (iii). In principle such motion could be made to vanish by going to sufficiently low temperatures. If case (iii) is responsible, however, it is difficult to understand why the "*O*" lines do not more closely represent a single quadrupole field.

The single observed *Y* quadrupole field at 100 K is closer in symmetry and magnitude to that observed for the *O* chains at higher temperatures. In fact, the new values of η and ν_Q are roughly halfway between the high-temperature *O* and *Y* values. This suggests the possibility that below the 59-K transition the two chains may present very similar quadrupole spectra. The test of this hypothesis is left as a subject for future studies.

The structural information[4] which suggests that the yellow and orange chains should be similar was, however, obtained at room temperature where the NQR data seem to show a marked difference between the two sites. This discrepancy can be reconciled in one or more of three simple ways. Firstly, our assignments for the sites may be wrong and in fact what we call *Y* is really Wilson's red chain. In this case the most notable effect of the transition is to cause the red chains to become more like the yellow and/or orange chains. Secondly, the differences may be due to the difference in the time scales of the NQR and diffraction experiments. Questions regarding the dynamics are best studied through their effect on the relaxation times and will be discussed later in this paper. The third possible explanation is that the differences seen in the NQR spectra simply do not appear in the structure. For example, differences in the conduction-electron wave functions between the two sites can greatly affect the quadrupole field (see Appendix) but may not be apparent in the structural study.

Above the transition the quadrupole field at the *Y* site, taking $\eta=0$, is described by $V_{zz}=-2V_{xx}=-2V_{yy}=\pm 0.93$ MHz, where we have incorporated the constants in Eq. (1) into the quadrupole-field tensor so that $V_{zz}=\nu_Q$. Below the transition (e.g., 100 K) we find $V_{zz}=-V_{xx}/(0.225)=-V_{yy}/(0.775)=\pm 1.13$ MHz. If we assume there is no change in the quadrupole-field principal axes then the change in the quadrupole field corresponds to the addition of an axial field in the *x*-*y* plane with a magnitude $\Delta\nu_Q=0.4$ MHz or about 40% the size of the field above the transition. Of course η may be as large as 0.25 above the transition and the principal axes may change below the transition; however, the change in the quadrupole field cannot be much smaller than 40% and may be much larger.

A small perturbation (e.g., the CDW) can cause a large change in the quadrupole field if there are two (or more) large contributions to the field which happen to cancel without the perturbation but do not cancel when the perturbation is present. The changes in the NQR positions of the "*Y*" lines are very rapid as a function of temperature (see Fig. 6) just below the transition at 145 K and are essentially complete by 100 K. However, the amplitude of the CDW (PLD) as measured by x-ray diffraction rises much more slowly as the temperature decreases.[5]

If the changes in the *Y* quadrupole field are due to a change in V_{lattice} [see Eq. (3)] we would expect the changes to follow the diffraction-intensity results. However, there is no simple, temperature-independent relationship between the diffraction results and the changes in the *Y* quadrupole field. Thus we assume the changes in the quadrupole field are due to changes in V_{local} which reflects the local electronic environment. The changes in the *Y* quadrupole field show essentially the same temperature dependence as the "fraction of the Fermi surface removed by the gap" determined by Ong and Monceau.[2] Since the quadrupole field is determined by all the conduction electrons—not just those at the Fermi surface—it is unclear to us why this relationship should exist.

It is interesting to note that recent studies of the CDW transition in the dichalcogenides also show a site where the quadrupole field changes from axial symmetry above the transition to a nonaxial ($\eta\neq 0$) symmetry below the transition.[36–38] In fact, if one plots this new value of η versus the transition temperature (see Fig. 8) one obtains a high degree of correlation between the results for the dichalcogenides and $NbSe_3$. We have no information at present to suggest that this correlation is more than coincidental. Correlations between the transition temperature and ionicity have been presented by Thompson for the dichalcogenides.[39]

D. Relaxation times

The relaxation times T_1 and T_2 were measured as discussed in Sec. III only to the extent necessary to help obtain a qualitative picture of the extent to which the changes in the NQR spectrum are static or dynamic. The measured values for the spin-spin relaxation rate $1/T_2$ for the highest-frequency transition of the nuclei at a *Y* site are shown in Fig. 9. All measurements were made at the point on the line shape where the signal was largest. The decay of the signal versus t_d was exponential at all the

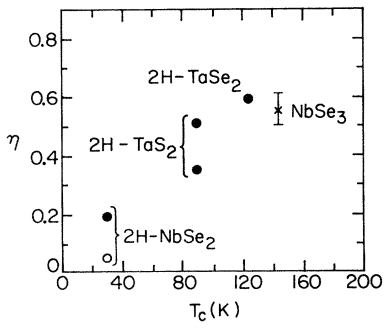

FIG. 8. "New" value of η (see text) for several chemically related CDW compounds vs the CDW transition temperature T_c. [2*H*-$TaSe_2$, Ref. 37; 2*H*-TaS_2, Ref. 36 (lower), and Ref. 37 (upper *and* lower); 2*H*-$NbSe_2$, open circle, Ref. 38 (closed circle is an estimate using Refs. 33 and 34); $NbSe_3$, this work].

temperatures measured. In contrast the decay of the signal at the O sites is more nearly Gaussian (convoluted with an exponential decay attributed to lifetime broadening by the spin-lattice relaxation) and the relaxation rate is slower ($T_2=600$ μs at room temperature) than at the Y sites. Since the linewidth of the O lines is much broader than $1/T_2$ there must be a significant broadening presumably due to a static distribution of quadrupole fields.

The decay characterized by T_2 may be exponential or Gaussian (or any shape with the same general form) if only static effects are important. If dynamics are important (i.e., the "motional-narrowing" regime) one is in the region of validity of Redfield theory.[19] In this case it is easy to show that the decay of the highest-frequency transition will be exponential. For a quadrupole field V which is axial on the average but has a fluctuating perturbation about the axial field $v(t)$, one has a contribution to the relaxation of the highest-frequency transition ($\frac{9}{2}\leftrightarrow\frac{7}{2}$),

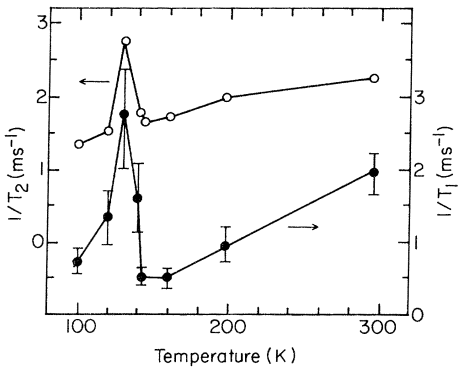

FIG. 9. Relaxation rates $1/T_2$ and $1/T_1$ for the yellow site as a function of temperature. Note the vertical scales have been offset slightly.

$$[1/T_2]_{\text{fluct}}=\{n_0\langle v_0v_0\rangle\tau_c+\langle v_1v_{-1}\rangle[n_1\tau_cf(4\omega_Q\tau_c)+n_1'\tau_cf(3\omega_Q\tau_c)]+\langle v_2v_{-2}\rangle[n_2\tau_cf(7\omega_Q\tau_c)+n_2'\tau_cf(5\omega_Q\tau_c)]\}h^{-2}\,, \tag{6}$$

where the components of the fluctuating field are related to the V_{ij} in Eq. (6) as in Ref. 19, $f(x)=(1+x^2)^{-1}$, and τ_c is the correlation time (exponential correlation function). The maximum of $\tau f(\omega\tau)$ occurs when $\tau=\omega^{-1}$. Here n and n' are numbers arising from the matrix elements of the angular-momentum operators. The first term on the right-hand side of Eq. (6) gives the effects of the secular part of the fluctuating field. The remainder of the terms are the effects of nonsecular (off-diagonal) terms and are closely related to the shift in the transition frequency calculated using second-order time-dependent perturbation theory. That is, when the nonsecular terms become important in the relaxation, e.g., $\tau\sim3\times10^{-8}$ s in our case, they may also give rise to a change in the transition frequency. Changes in the line shape due to the secular term begin to be apparent when $\tau\leq h\,|v_0|$ or about 10^{-6} s in our case. This motional-narrowing process will be discussed further later on in this section.

The spin-lattice relaxation rate $1/T_1$ is not so simply analyzed. Results for measurements of T_1 for the $\frac{9}{2}\leftrightarrow\frac{7}{2}$ transition of nuclei in the Y sites are summarized in Fig. 9. The decay of the signal versus t_w consists of the sum of several exponentials.[40] Experimentally we determined T_1 from the initial decay of the signal from its maximum to about 60% of the maximum at which point a second exponential takes hold.

To calculate $1/T_1$ using Redfield theory is somewhat complicated. However, qualitatively the contributions to $1/T_1$ due to a fluctuating quadrupole field will have the same general features as the nonsecular part of $1/T_2$. Since $NbSe_3$ is a metal there is a further complication in that relaxation by the conduction electrons' magnetic moments may be important. This contribution to $1/T_1$ will have the form[19]

$$1/T_1\propto\rho^2(E_f)T\,, \tag{7}$$

where $\rho(E_f)$ is the density of states at the Fermi surface and T is the temperature. This contribution to the relaxation will, of course, also contribute to $1/T_2$.

If a band gap at the Fermi surface accompanies the CDW, as is to be expected, and the relaxation is described by Eq. (7), then one would expect $1/T_1$ to be much smaller below the CDW transition than above. This is what is observed at the O sites where limited measurements of T_1 show roughly an order-of-magnitude decrease in $1/T_1$ between 160 and 100 K.[41]

At the Y sites $1/T_1$ appears to decrease a bit faster than the temperature down to the transition where it increases and then decreases in a manner similar to $1/T_2$. The facts that the T_2 decay at the Y sites is exponential while at the O sites it is Gaussian, and that there are peaks in both $1/T_1$ and $1/T_2$ versus temperature, show the presence of a changing fluctuating field at the Y sites.

We attribute the overall slope of the two types of relaxation versus temperature for the Y sites, aside from the peak in the vicinity of 130 K, to relaxation by the conduction electrons though other causes cannot be ruled out. The fact that the peaks in $1/T_1$ and $1/T_2$ occur simultaneously with the large changes in the line shape show that the changes in the line shape are closely related to changes in the fluctuating field. Note that the changes in the fluctuating field should not be compared *a priori* with the critical fluctuations that one might expect near a phase transition since the fluctuations discussed here are not necessarily long range and are not necessarily of the order parameter.

We now show that the change in the Y-line positions and the change in the relaxation may arise from the same

fluctuating field. The quadrupole field Hamiltonian H_Q at a given Y site can be written as the sum of three contributions,

$$H_Q = H_Q^0 + H_Q'(T) + H_Q''(\tau) , \tag{8}$$

where H_Q^0 is essentially independent of temperature and is what is observed in the normal state (above 145 K), H_Q' is a static contribution which depends on temperature T, and H_Q'' is a dynamic contribution with an amplitude and characteristic time τ which may depend on temperature. Either H_Q' or H_Q'' alone can be used to describe the changes in the average line positions but only H_Q'' will contribute to the relaxation rates. Line changes due to changes in H_Q' are easily understood. However, since our lines broaden near the transition, to interpret our data we would require an additional broadening mechanism—for example, a distribution in H_Q' due perhaps to a distribution of transition temperatures—throughout our sample. As discussed following Eq. (6), changes in the line positions due to H_Q'' occur when τ becomes long enough so that H_Q'' is effectively static. For short values of τ the NQR spectra will reflect only the time-averaged field so that even though H_Q'' may be present, it may not be observable. This averaging of a fluctuating field is referred to as "motional averaging" or motional narrowing. In the transition region from short to long τ, motional-narrowing theory predicts a broadening of the NQR line—no additional broadening is required to interpret our data. While by definition H_Q' will vanish above the transition, H_Q'' need not vanish.

Our relaxation data indicate that a fluctuating field, i.e., H_Q'', is present. One would like to know if H_Q', a static contribution, is also present. We will now present a simple calculation which shows that we do not need H_Q' in order to understand our data. We assume the changes in the line position are only due to the motional-narrowing process and show that we obtain reasonable agreement with the relaxation data.

Earlier in this paper we calculated a change in the Y quadrupole field which we now assume is the amplitude of H_Q''. That is, we write

$$|H_Q''| = 0.4 \text{ MHz}(3I_x^2 - I^2)/6 . \tag{9}$$

The changes in the NQR spectrum are assumed to be only due to a change in τ. The fluctuations of H_Q'' are such that an average over time of $H_Q''(t)$ vanishes. Equation (9) alone for the *fluctuating* field does not yield the observed changes in the line positions since one cannot find a *single* value of V_{zz} which changes with changing τ which also vanished for a time average. However, because of its simplicity we will use Eq. (9) to obtain an estimate of the relaxation time T_2. An example of a field which does not give the required change in line position would be characterized by $V_{z'z'} = -V_{x'x'}/(0.225) = -V_{y'y'}/(0.775) = 1.13$ MHz where the z' axis makes an angle of roughly 20° with the z axis of the axial field. To determine this angle more precisely requires knowledge of the sense of the rotation with respect to x' and y' and the value of η above the transition. The fluctuations would then correspond to rotations about the z axis—either continuously or in discrete steps. Relaxation due to this more correct choice will be as much as an order of magnitude slower than that of the field described by Eq. (9) due mainly to the differences in the numerical factors n_1 and n_2 in Eq. (6).

Setting Eq. (9) in Eq. (6) we find a minimum relaxation time of $T_2 \sim 20$ μs when $1/\tau$ is roughly equal to the transition frequency. Nuclei with a relaxation time this fast would not be observable. At 130 K the relaxation time was measured at the highest point on the line shape (4.3 MHz) and thus is biased toward longer relaxation times (longer τ's). It would not be unreasonable for this measurement—judging by the temperature dependence of the line positions and using simple motional-narrowing theory[19]—that $1/\tau$ is 1 or even 2 orders of magnitude away from the transition frequency, giving a calculated relaxation time within an order of magnitude of what we observe. We can conclude that the size of the fluctuating field is at least comparable to the changes we observe in the quadrupole field between high and low (~ 100 K) temperatures.

At present we can understand data using only H_Q''—H_Q' is not needed. Of course a more rigorous test of whether H_Q' is present or not is necessary before a definite conclusion is reached. Such a test may involve measurements of the principal axes above and below the transition (to obtain accurate values for the changes in the quadrupole field) and/or the measurement of the frequency dependence(s) of the relaxation time(s) (to obtain an independent measurement of τ). It is not clear whether the dynamics we observe are related to the dynamics observed by Fung and Steeds.[12]

V. SUMMARY

A study of the ^{93}Nb NQR spectrum between 100 and 300 K and 2.6–5.3 MHz shows two quadrupole fields. The third site expected on the basis of the crystal structure has not been observed. One of the observed sites is nearly antiaxial ($\eta \approx 1$) and shows changes which are more or less what one would expect in the presence of a CDW at the CDW transition. Dynamics do not appear to be important at this site. The second observed site is nearly axial ($\eta \approx 0$) above the transition and appears to be a single quadrupole field roughly halfway between axial and antiaxial below the transition. The changes in this second site below the CDW transition are much more pronounced than the first and do not follow the temperature dependence of the PLD measured with diffraction techniques. Dynamics are very important at this site and we show that the amplitude of the dynamics is large enough so that the change in the observed quadrupole field may be due solely to changes in the dynamics of the quadrupole field at that site.

Based on a simple calculation we tentatively associate the antiaxial, axial, and unobserved sites, respectively, with Wilson's orange, yellow, and red sites. Wilson's proposals that the transition at 145 K should be associated with a single site (the yellow site) and that the incommensurate CDW will be in a quasicommensurate state do not

explain our observations. The situation present in $NbSe_3$ is evidently somewhat more complicated than Wilson's picture.

Note added in proof. Joseph H. Ross, Jr. and Zhiyue Wang of our laboratory have recently observed the ^{93}Nb resonance of a sample consisting of a large number of oriented single crystals of $NbSe_3$ using static magnetic fields from 20 to 60 kG. They observe all three Nb chains. None of their preliminary results conflict with the findings of our paper.

ACKNOWLEDGMENTS

The authors are grateful to Professor John Bardeen for his stimulus and help, and to Joseph H. Ross, Jr. and Zhiyue Wang for their assistance. This work was supported by the U. S. Department of Energy, Division of Materials Sciences, under Contract No. DE-AC02-76ER01198.

APPENDIX

In this appendix the results of a general calculation of the quadrupole field due to local electrons are presented. The charge density $\rho(r)$ is expanded about a nuclear position ($\vec{r}=\vec{0}$) as

$$\rho(\vec{r})=\sum_{l,m,l',m'} A_{lml'm'} Y_l^m(\theta,\phi) Y_{l'}^{m'*}(\theta,\phi) f_{lm}(r) f^*_{l'm'}(r) , \tag{A1}$$

where the $A_{lml'm'}$ are the expansion coefficients, Y_l^m is a spherical harmonic, and $f_{lm}(r)$ contains the radial dependence. Roughly speaking, this expansion corresponds to an averaged wave function squared. The quadrupole field due to a unit charge located at $\vec{r}=(x_1,x_2,x_3)$ is given by[19]

$$V_{ij}=\frac{3x_ix_j-\delta_{ij}r^2}{r^5} . \tag{A2}$$

The total quadrupole field is then given by the sum over all the charge density. This can be done readily with the result

$$V''_m=\sum_{l,m,l',m'} -eg''_m\langle 1/r^3\rangle_{lml'm'} A_{lml'm'} \frac{(2l+1)^{1/2}}{(2l'+1)^{1/2}} \left[\frac{5}{4\pi}\right]^{1/2} \langle l200\,|\,l2l'0\rangle\langle l2mm''\,|\,l2l'm'\,|\,\rangle , \tag{A3}$$

where m'' is an integer, $-2\leq m''\leq 2$, $-e$ is the charge of an electron, g''_m is $(16\pi/5)^{1/2}$ for $m''=0$ and $(24\pi/5)^{1/2}$ otherwise, $\langle 1/r^3\rangle_{lml'm'}$ is the result of the radial integral which in many cases will not depend on m and m', and the last two terms in angular brackets are Clebsch-Gordan coefficients. The relation used between the V_m and the V_{ij} in Eq. (1) is given by Slichter.[19]

Owing to the "selection rules" of the Clebsch-Gordan coefficients, many of the $A_{lml'm'}$ will not contribute to the quadrupole field at all.

If only d-like orbits are important and one uses coordinates corresponding to a set of principal axes, then one has $\eta=(V_2+V_{-2})/V_0$ and $V_{\pm 1}=0$. Expressed in a more convenient manner this gives (in units of $-e\langle 1/r^3\rangle$

$$V_0=\tfrac{4}{7}(\rho_{3z^2-r^2}-\rho_{x^2-y^2}-\rho_{xy})+\tfrac{2}{7}(\rho_{yz}+\rho_{xz}) \tag{A4}$$

and

$$V_2+V_{-2}=\tfrac{6}{7}(\rho_{yz}-\rho_{xz})-\frac{2\sqrt{6}}{7}(A_{2022}+A_{2220}+\text{c.c.}) , \tag{A5}$$

where ρ_x is the probability that the wave function α is occupied by an electron and c.c. denotes the complex conjugate.

*Present address: Department of Materials Science, University of Pennsylvania, Philadelphia, PA 19104.

[1]P. Haen, P. Monceau, B. Tissier, G. Waysand, A. Meerschaut, P. Molinie, and J. Rouxel, in *Proceedings of the Fourteenth International Conference on Low Temperature Physics, Otaniemi, Finland, 1975,* edited by M. Krusius and M. Vuorio (North-Holland, Amsterdam, 1975), Vol. 5, p. 445; J. Chaussy, P. Haen, J. C. Lasjaunias, P. Monceau, G. Waysand, A. Waintel, A. Meerschaut, P. Molinie, and J. Rouxel, Solid State Commun. 20, 759 (1976).

[2]N. P. Ong and P. Monceau, Solid State Commun. 20, 759 (1978); Phys. Rev. B 16, 3443 (1977).

[3]K. Tsutsumi, T. Takagaki, M. Yamamoto, Y. Shiozaki, M. Ido, T. Sambongi, K. Yamaya, and Y. Abe, Phys. Rev. Lett. 39, 1675 (1977).

[4]J. L. Hodeau, M. Marezio, C. Roucau, A. Ayroles, A. Meerschaut, J. Rouxel, and P. Monceau, J. Phys. C 11, 4117 (1978).

[5]R. M. Fleming, D. E. Moncton, and D. B. McWhan, Phys. Rev. B 18, 5560 (1978).

[6]P. Monceau, N. P. Ong, A. M. Portis, A. Meerschaut, and J. Rouxel, Phys. Rev. Lett. 37, 602 (1976).

[7]R. M. Fleming and C. C. Grimes, Phys. Rev. Lett. 42, 1423 (1979).

[8]J. W. Brill, N. P. Ong, J. C. Eckert, J. W. Savage, S. K. Khanna, and R. B. Somoano, Phys. Rev. B 23, 1517 (1981).

[9]G. Gruner, A. Zawadowski, and P. M. Chaikin, Phys. Rev. Lett. 46, 511 (1981).

[10]J. C. Gill, Solid State Commun. 37, 459 (1981); 44, 1041 (1982).

[11]H. Frohlich, Proc. R. Soc. London Ser. A 223, 296 (1953).

[12]K. K. Fung and J. W. Steeds, Phys. Rev. Lett. 45, 1696 (1980).
[13]A. Meerschaut and J. Rouxell, J. Less-Common Metals 39, 197 (1975).
[14]J. A. Wilson, Phys. Rev. B 19, 6456 (1979).
[15]D. W. Bullett, J. Phys. C 15, 3069 (1982).
[16]T. P. Das and E. L. Hahn, in *Solid State Physics,* Suppl. 1, edited by F. Seitz and D. Turnbull (Academic, New York, 1958).
[17]E. N. Kaufmann and R. J. Vianden, Rev. Mod. Phys. 51, 161 (1979).
[18]M. H. Cohen, Phys. Rev. 96, 1278 (1954).
[19]C. P. Slichter, *Principles of Magnetic Resonance,* second revised and expanded edition, corrected second printing (Springer, New York, 1980).
[20]N. Karnezos, L. B. Welsh, and M. W. Shafer, Phys. Rev. B 11, 1808 (1975).
[21]E. Ehrenfreund, A. C. Gossard, and F. R. Gamble, Phys. Rev. B 5, 1708 (1972).
[22]One could argue that there are contributions to the quadrupole field from the lattice which cancel due to the hexagonal symmetry at an Nb site in $NbSe_2$ which will not cancel in $NbSe_3$. However, the change in the quadrupole field in $NbSe_2$ when distorted from hexagonal symmetry by a CDW is relatively small (see Refs. 34 and 38).
[23]R. V. Pound, Phys. Rev. 79, 685 (1950).
[24]See H. E. Rhodes, P. K. Wang, H. T. Stokes, C. P. Slichter, and J. H. Sinfelt, Phys. Rev. B 26, 3559 (1982).
[25]A. Abragam, *The Principles of Nuclear Magnetism* (Clarendon, Oxford, 1956).
[26]For $\eta=1$ the lower-frequency transition is essentially a spin-$I=1$ problem while the upper consists of two independent spin-$\frac{1}{2}$ problems.
[27]N. Bloembergen and T. J. Rowland, Acta Metall. 1, 731 (1953).
[28]M. H. Cohen and F. Reif, in *Solid State Physics,* edited by F. Seitz and D. Turnbull (Academic, New York, 1957), Vol. 5, p. 321.
[29]For example, see J. D. Jackson, *Classical Electrodynamics* (Wiley, New York, 1962).
[30]For a discussion of this method, see A. Avogadro, G. Bonera, and M. Villa, J. Magn. Res. 35, 316 (1964).
[31]G. H. Stauss, J. Chem. Phys. 40, 1988 (1964).
[32]J. A. R. Stiles and D. L. Williams, J. Phys. C 9, 3941 (1976).
[33]C. Berthier, D. Jerome, and P. Molinie, J. Phys. C 11, 797 (1978).
[34]M. C. Chen, Ph.D. thesis, University of Illinois, 1982 (unpublished); M. C. Chen and C. P. Slichter, Phys. Rev. B 27, 278 (1983).
[35]D. Follstaedt and C. P. Slichter, Phys. Rev. B 13, 1017 (1976).
[36]T. Butz, A. Hubler, A. Lerf, and W. Biberacher, Mat. Res. Bull. 16, 541 (1982); T. Butz, in The Satellite Meeting on Charge Density Waves and Related Phenomena of the 2nd General Conference of the Condensed Matter Division of the European Physical Society, Manchester, United Kingdom, 1983 (unpublished).
[37]H. Nishihara, in The Satellite Meeting on Charge Density Waves and Related Phenomena of the 2nd General Conference of the Condensed Matter Division of the European Physical Society, Manchester, United Kingdom, 1982 (unpublished). See also N. Nishihara, G. A. Scholz, and R. F. Frindt, Solid State Commun. 44, 507 (1982); H. Nishihara, G. A. Scholz, M. Naito, R. F. Frindt, and S. Tanaka, J. Magn. Magn. Mater. 31-34, 717 (1983).
[38]E. Ehrenfreund, A. C. Gossard, F. R. Gamble, and T. H. Geballe, J. Appl. Phys. 42, 1491 (1971).
[39]A. H. Thompson, Phys. Rev. Lett. 34, 520 (1975).
[40]D. E. MacLaughlin, J. D. Williamson, and J. Butterworth, Phys. Rev. B 4, 60 (1971).
[41]J. H. Ross, Jr. (private communication).